SUPPLEMENTARY MATERIAL

CYP11A1-derived vitamin D_3 products protect against UVB-induced inflammation and promote keratinocytes differentiation

Anyamanee Chaiprasongsuk[1, 2, 6], Zorica Janjetovic[1], Tae-Kang Kim[1], Robert C. Tuckey[3], Wei Li[4], Chander Raman[5], Uraiwan Panich[6], Andrzej T. Slominski[1, 7*]

[1]Department of Dermatology, [5]Department of Medicine and Microbiology, Division of Clinical Immunology and Rheumatology, University of Alabama at Birmingham, Birmingham, AL, USA, [2]Faculty of Medicine and Public Health, HRH Princess Chulabhorn College of Medical Science, Chulabhorn Royal Academy, Bangkok, Thailand, [3]School of Molecular Sciences, The University of Western Australia, Perth, WA, Australia, [4]Department of Pharmaceutical Sciences, University of Tennessee Health Science Center, Memphis, TN, USA, [6]Department of Pharmacology, Faculty of Medicine Siriraj Hospital, Mahidol University, Bangkok, Thailand, [7]VA Medical Center, Birmingham, AL, USA.

*Corresponding author:

Andrzej T. Slominski, MD, PhD, Department of Dermatology, University of Alabama at Birmingham, Birmingham, AL 35249. USA; e-mail: aslominski@uabmc.edu; phone: 205.934.5245

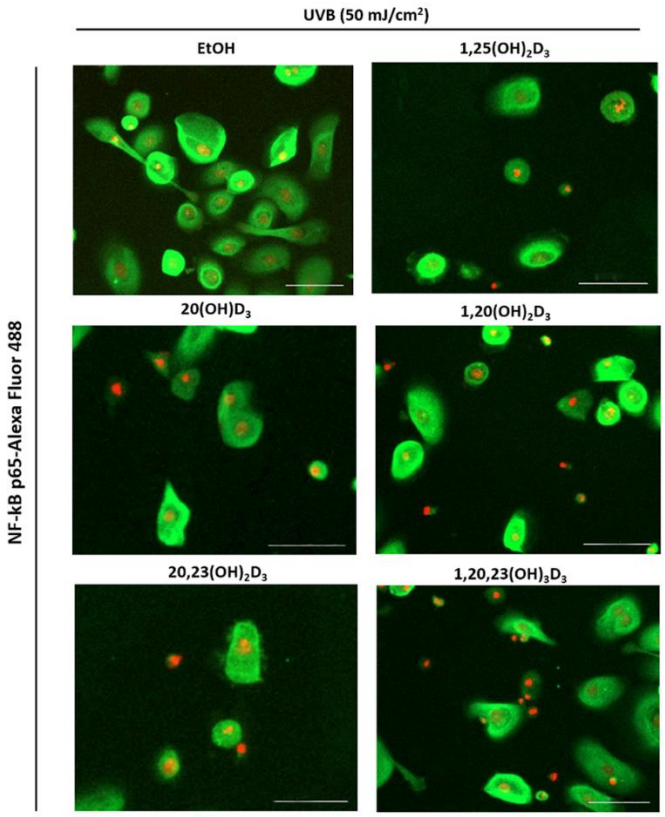

Supplementary Figure S1. Immunofluorescent images of UVB-irradiated cells treated with vitamin D_3 hydroxyderivatives: nuclear/cytosolic NF-κB p65 detection

Keratinocytes were pretreated individually with 100 nM of each of the hydroxyderivatives (or ethanol vehicle), for 24 h before UVB irradiation (50 mJ/cm^2) then further incubated with the same hydroxyderivative for an additional 24 h. Cells were fixed and stained with anti-NF-κB p65 antibody and imaged with a fluorescence microscope. Immunofluorescent cells show the NF-κB p65 levels in UVB-irradiated cells treated with the indicated secosteroid. Keratinocytes stained with NF-κB p65 antibody exhibited green fluorescence while nuclear staining with propidium iodine caused red fluorescence. Immunofluorescent positive cells were captured using the Cytation™ 5 cell imaging, n ≥ 100 cells for each condition. Scale bar = 100 μm. The immunofluorescent images are representative pictures for the immunofluorescent graph analysis.

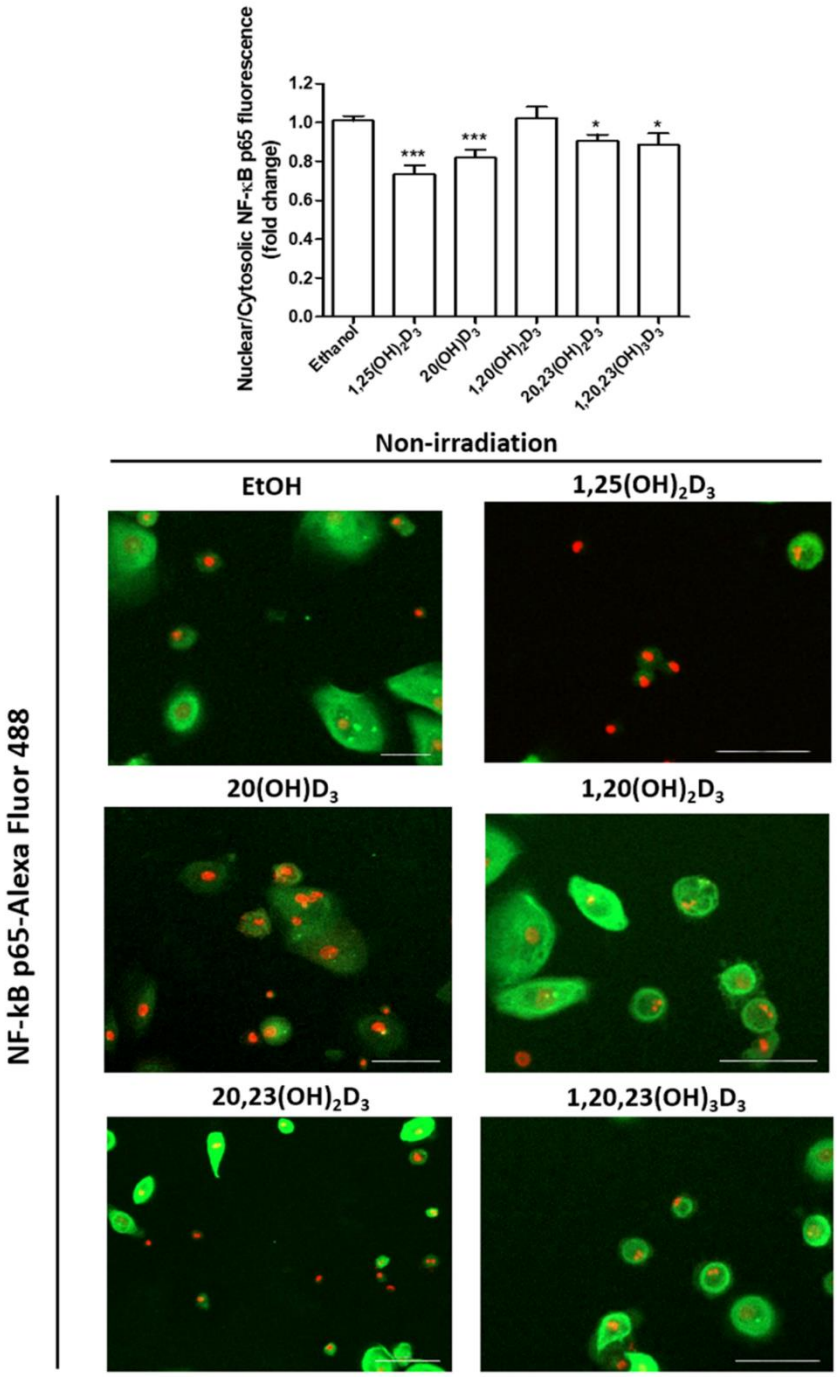

Supplementary Figure S2. Immunofluorescent images of non-irradiated cells treated with hydroxyderivatives of vitamin D_3: nuclear/cytosolic NF-κB p65 detection

Keratinocytes were incubated with the indicated hydroxyderivative (100 nM), or ethanol vehicle, for 24 h. Cells were fixed and stained with anti-NF-κB p65 antibody and imaged with a

fluorescence microscope. Fluorescence intensity was measured using the Cytation 5 reader and data were analyzed using Graph Pad Prizm. Images and graphs show the levels of fluorescence intensities in non-irradiated cells with the effects of the hydroxyderivatives shown in the graph (upper panel) and images in the lower panels. Keratinocytes stained with NF-κB p65 antibody exhibited green fluorescence while nuclear staining with propidium iodine caused red fluorescence. Data are presented as the ratio (mean ± SD) nuclear/cytoplasmic staining calculated from fluorescence intensities. Immunofluorescent positive cells were captured using the Cytation™ 5 cell imaging, $n \geq 100$ cells for each condition. Scale bar = 100 µm. The statistical significance of differences was evaluated using the student t-test, * $P < 0.05$ and *** $P < 0.001$, for all conditions. The immunofluorescent images are representative pictures for the immunofluorescent graph analysis.

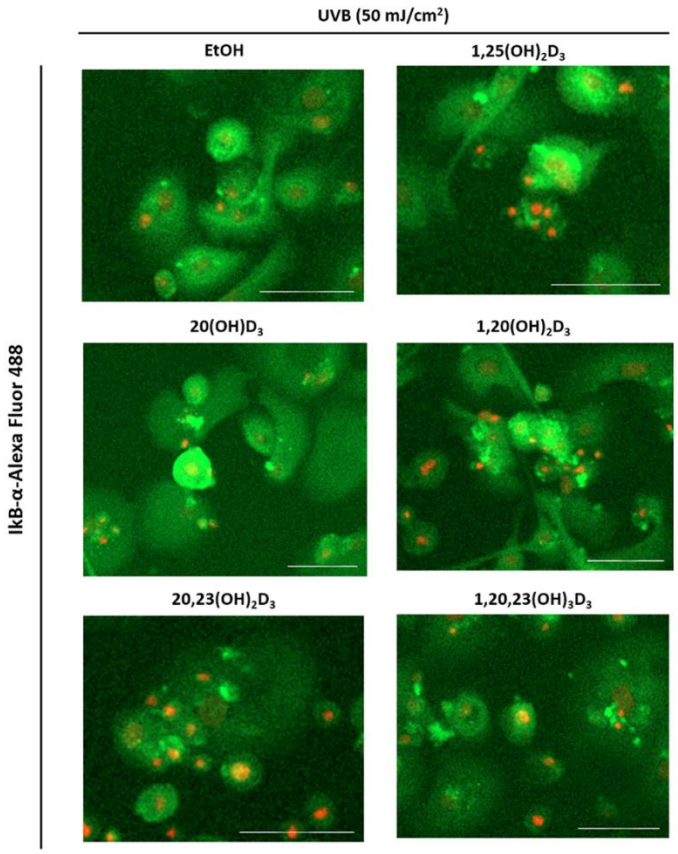

Supplementary Figure S3. Immunofluorescent images of UVB-irradiated cells treated with hydroxyderivatives of vitamin D_3: cytosolic-IκB-α detection

Keratinocytes were pretreated individually with each of the indicated vitamin D_3 hydroxyderivatives (100 nM) or ethanol vehicle, for 24 h before UVB irradiation (50 mJ/cm^2) then further incubated with the same hydroxyderivative for an additional 24 h. Cells were fixed and stained with anti-IκB-α antibody and imaged with a fluorescence microscope. Immunofluorescent cells show the IκB-α levels in UVB-irradiated cells treated with the indicated secosteroid. Keratinocytes stained with IκB-α antibody exhibited green fluorescence while nuclear staining with propidium iodine caused red fluorescence. Immunofluorescent positive cells were captured using the Cytation™ 5 cell imaging, n ≥ 100 cells for each condition. Scale bar = 100 µm. The immunofluorescent images are representative pictures for the immunofluorescent graph analysis.

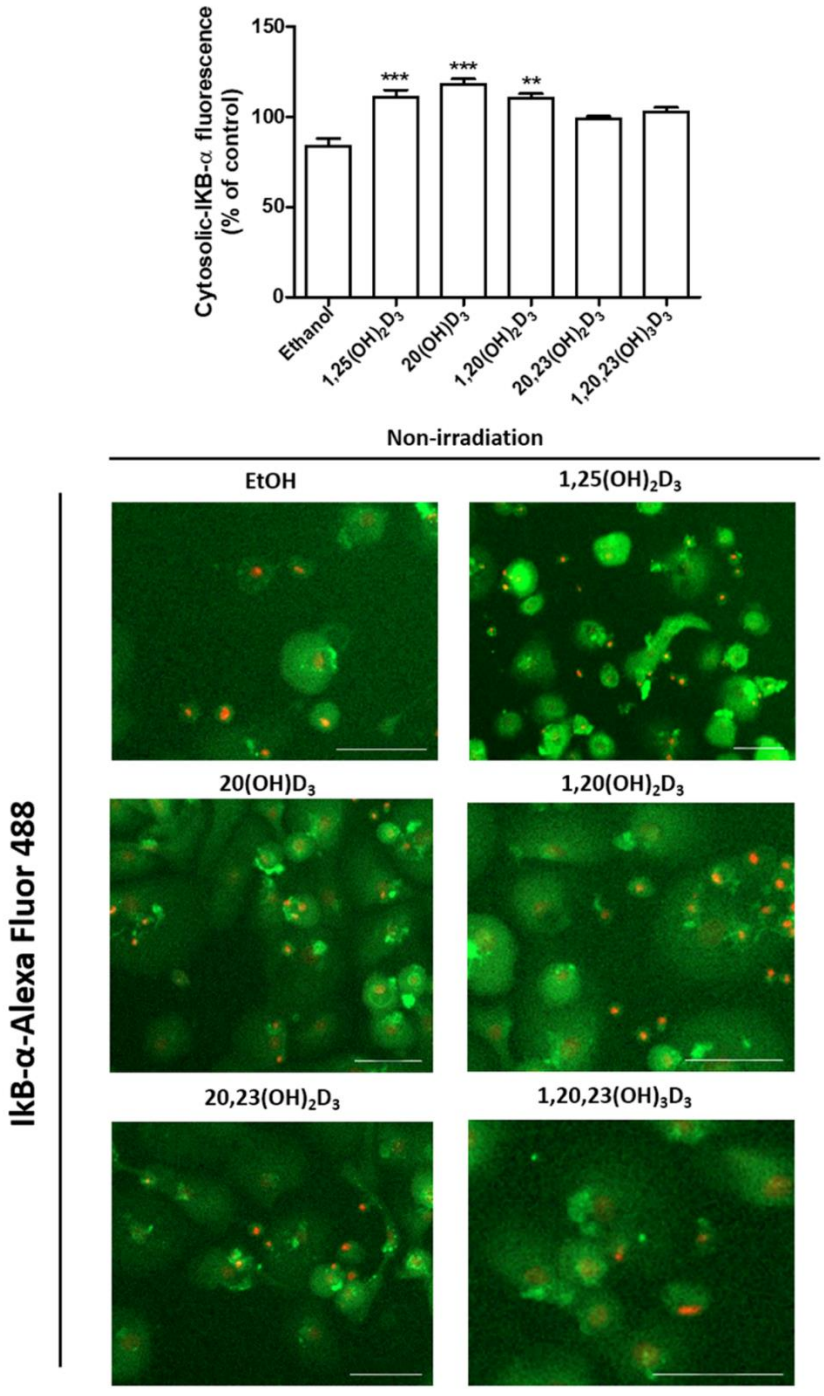

Supplementary Figure S4. Immunofluorescent images of non-irradiated cells treated with hydroxyderivatives of vitamin D_3: cytosolic-IκB-α detection

Keratinocytes were incubated with the indicated hydroxyderivative (100 nM) or ethanol vehicle, for 24 h. Cells were fixed and stained with anti-IκB-α antibody and imaged with a fluorescence microscope. Fluorescence intensity was measured using the Cytation 5 reader and data were analyzed using Graph Pad Prizm. Images and graphs show the levels of fluorescence intensities in non-irradiated cells with the effects of the hydroxyderivatives shown in the graph (upper panel) and images in the lower panels. Keratinocytes stained with IkB-α antibody exhibited green fluorescence while nuclear staining with propidium iodine caused red fluorescence. Immunofluorescent positive cells were captured using the Cytation™ 5 cell imaging, $n \geq 100$ cells for each condition. Scale bar = 100 µm. Data are presented as the ratio (mean ± SD) nuclear/cytoplasmic staining calculated from fluorescence intensities. The statistical significance of differences was evaluated using the student t-test, ** $P < 0.01$ and *** $P < 0.001$, for all conditions. The immunofluorescent images are representative pictures for the immunofluorescent graph analysis.

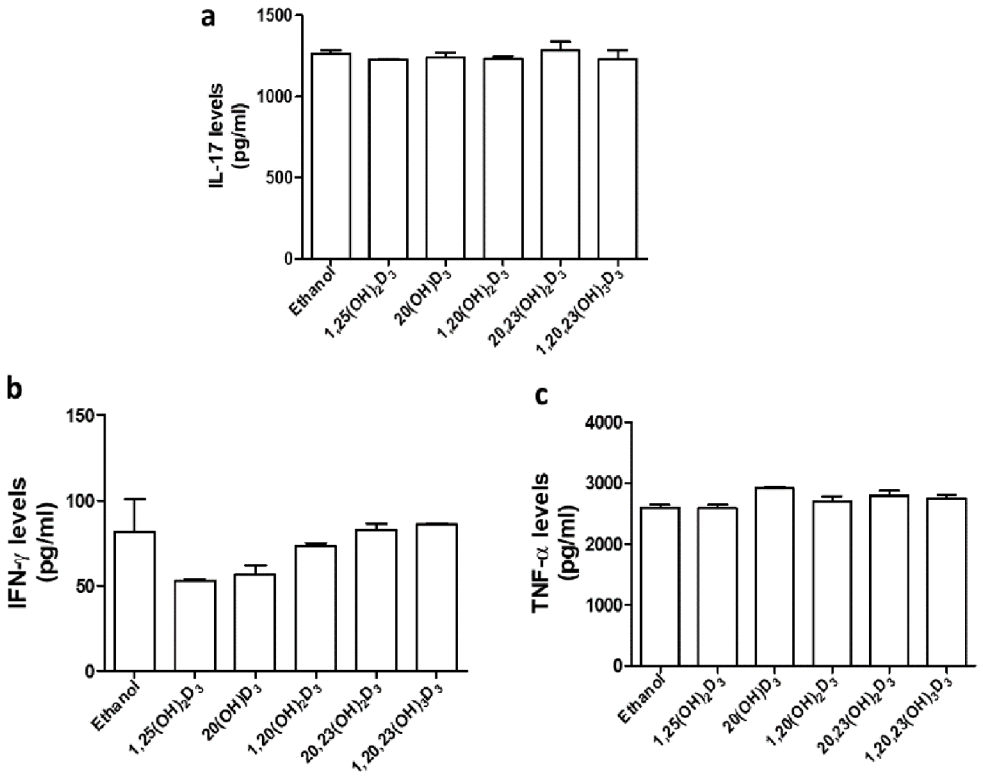

Supplementary Figure S5. The levels of IL-17, IFN-γ, and TNF-α in non-irradiated cells treated with hydroxyderivatives of vitamin D_3

Keratinocytes were incubated with the indicated hydroxyderivative (100 nM) or ethanol vehicle, for 24 h prior to UVB irradiation (50 mJ/cm^2). Cell supernatants were plated using an ELISA assay kit tagged with (a) IL-17, (b) IFN-γ, and (c) TNF-α antibody. The cytokine levels of secosteroid-treated cells compared to vehicle-treated cells are presented as bar graphs. The levels of inflammatory cytokines (pg/ml) were calculated from protein standards. The statistical significance of differences was evaluated by the student t-test, for all conditions.

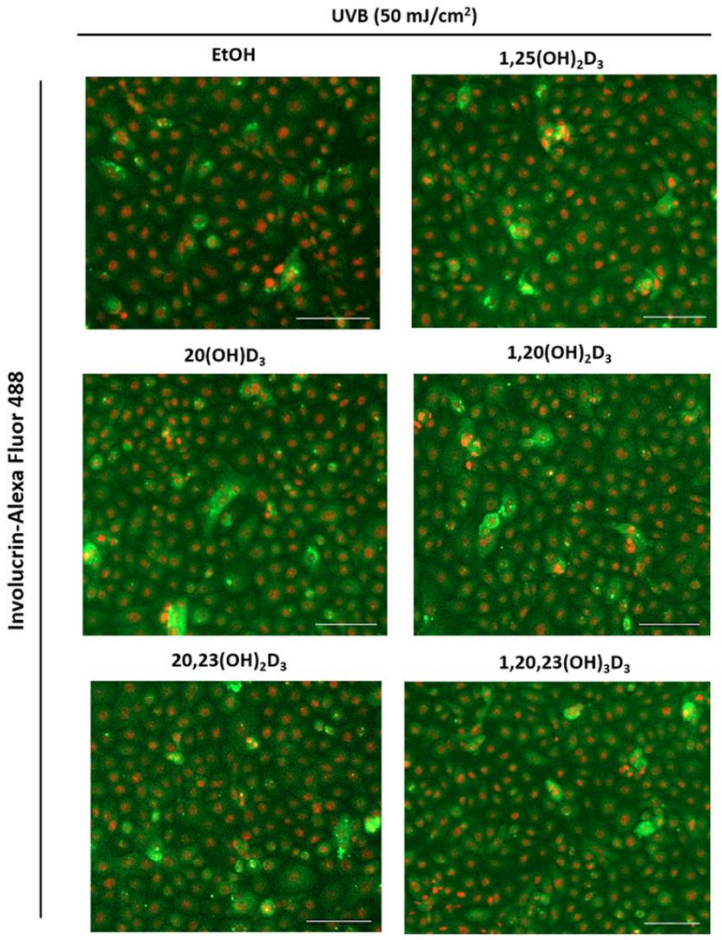

Supplementary Figure S6. Immunofluorescent images of UVB-irradiated cells treated with hydroxyderivatives of vitamin D_3: involucrin (IVL) detection

Keratinocyte were pretreated individually with 100 nM of each of the indicated hydroxyderivatives (or ethanol vehicle) for 24 h before UVB irradiation (50 mJ/cm^2), then further incubated with the same hydroxyderivative for an additional 24 h. Cells were fixed and stained with anti-IVL antibody and imaged with a fluorescence microscope. Immunofluorescent cells show the IVL levels in UVB-irradiated cells treated with the indicated secosteroid. Keratinocytes stained with IVL antibody exhibited green fluorescence while nuclear staining with propidium iodine caused red fluorescence. Immunofluorescent positive cells were captured using the Cytation™ 5 cell imaging,

$n \geq 100$ cells for each condition. Scale bar = 100 μm. The immunofluorescent images are representative pictures for the immunofluorescent graph analysis.

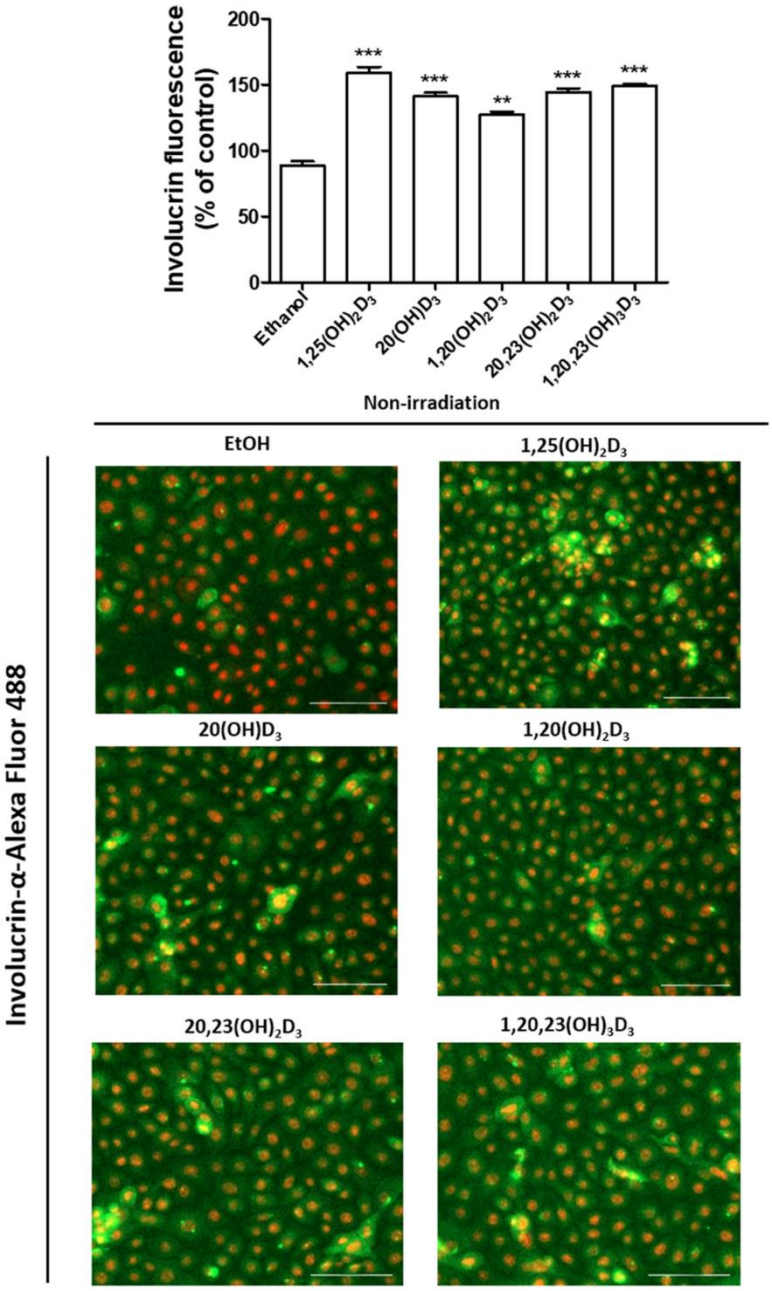

Supplementary Figure S7. Immunofluorescent images of non-irradiated cells treated with hydroxyderivatives of vitamin D_3: involucrin (IVL) detection

Keratinocytes were incubated with the indicated hydroxyderivative (100 nM) or with ethanol vehicle, for 24 h. Cells were fixed and stained with anti-IVL antibody and imaged with a

fluorescence microscope. Fluorescence intensity was measured using the Cytation 5 reader and data were analyzed using Graph Pad Prizm. Images and graphs show the levels of fluorescence intensities in non-irradiated cells with the effects of the hydroxyderivatives shown in the graph (upper panel) and images in the lower panels. Keratinocytes stained with IVL antibody exhibited green fluorescence while nuclear staining with propidium iodine caused red fluorescence. Immunofluorescent positive cells were captured using the Cytation™ 5 cell imaging, $n \geq 100$ cells for each condition. Scale bar = 100 μm. Data are presented as the ratio (mean ± SD) nuclear/cytoplasmic staining calculated from fluorescence intensities. The statistical significance of differences was evaluated using the student t-test, * $P < 0.05$ and *** $P < 0.001$, for all conditions. The immunofluorescent images are representative pictures for the immunofluorescent graph analysis.

Supplementary Table S1. Sequences of primers used in the heat map analysis

Additional details are in [1-6].

Function	Gene	Description	Sequence (L and R)
The biological actions of vitamin D_3	*VDR*	Vitamin D_3 receptor	CTTACCTGCCCCCTGCTC AGGGTCAGGCAGGGAAGT
Inflammation	*TLR4*	Toll-like receptor 4	CAG GTG GAA TTG TAT CGC CT CGA GGC TTT TCC ATC CAA TA
	COX2	Cyclooxygenase-2	GAATGGGGTGATGAGCAGTT CAGAAGGGCAGGATACAGC
	ICAM	Intracellular adhesion molecule	CCTTCCTCACCGTGTACTGG AGCGTAGGGTAAGGTTCTTGC
	IL-6	Interleukin 6	GAAGCTCTATCTCGCCTCCA AGCAGGCAACACCAGGAG
	IL-8	Interleukin 8	AGACAGCAGAGCACACAAGC ATGGTTCCTTCCGGTGGT
	IL-17	Interleukin 17	TGGGAAGACCTCATTGGTGT GGATTTCGTGGGATTGTGAT
	IL-33	Interleukin 33	TGTCAACAGCAGTCTACTGTGGAGTGCT GCAAAAGTAATGGATTGATCATTGTA

	IL-1α	Interleukin 1 alpha	GGTTGAGTTTAAGCCAATCCA TGCTGACCTAGGCTTGATGA
	IL-1β	Interleukin 1 beta	CRGTCCTGCGTGTTGAAAGA TTGGGTAATTTTTGGGATCTACA
	IL-10	Interleukin 10	TGGGGGAGAACCTGAAGAC CCTTGCTCTTGTTTTCACAGG
	CD14	Cluster of differentiation 14	GTTCGGAAGACTTATCGACCAT ACAAGGTTCTGGCGTGGT
	NFkB p50	nuclear factor kappa B p50	ACCCTGACCTTGCCTATTTG AGCTCTTTTTCCCGATCTCC
	NFkB p65 (RelA)	nuclear factor kappa B p65 (RelA)	CGGGATGGCTTCTATGAGG CTCCAGGTCCCGCTTCTT
	IkB-α	Inhibitory-kappa B-alpha	GTCAAGGAGCTGCAGGAGAT GATGGCCAAGTGCAGGAA
	bcl2	B-cell lymphoma 2	AGTACCTGAACCGGCACCT GGCCGTACAGTTCCACAAA
	BNIP	BCL2 adenovirus E1B interacting	CCGGGATGCAGGAGGAGAG TTATAAATAGAAACCGAGGCTGGAAC
Differentiation	*IVL*	Involucrin	TGCCTCAGCCTTACTGTGAGT TCATTTGCTCCTGATGGGTA

	LOR	Loricrin	GTGGGAGCGTCAAGTACTCC AGAGTAGCCGCAGACAGAGC
	FLG	Filaggrin	GGCACTCATCATGCAGAGAA ATGGTGTCCTGACCCTCTTG
	TGM1	Transglutaminase	TCTGTGGGTCCTGTCCCATCCATCCTGACC CCCCAACGGCCCACATCGGAACGTGGCCCATCCATCATGC
	KRT1	Cytokeratin 1	GTTCCAGCGTGAGGTTTGTT TAAGGCTGGGACAAATCGAC
	KRT10	Cytokeratin 10	GGCTCTGGAAGAATCAAACTATGAGC GGATGTTGGCATTATCAGTTGTTAGG
	KRT14	Cytokeratin 14	CTGTCTCCCGCACCAGCTTCACCTCC CTCCACAAGCACCCGCAAGGCTGACC
	FGF23	Fibroblast growth factor 23	CAGCATGAGCGTCCTCAGAG GCCAGCATCCTCTGATCTGATC
House-keeping genes	*β-actin*	β-actin	CCAACCGCGAGAAGATGA CCAGAGGCGTACAGGGATAG
	CYCB	cyclophillin B	TGTGGTGTTTGGCAAAGTTC GTTTATCCCGGCTGTCTGTC
	GAPDH	Glyceraldehyde-3-Phosphate Dehydrogenase	AGCCACATCGCTCAGACAC GCCCAATACGACCAAATCCC

REFFERNCES FOR SUPPLEMENTARY MATERIAL

[1] R. Aoki, A. Aoki-Yoshida, C. Suzuki, Y. Takayama, Protective effect of indole-3-pyruvate against ultraviolet b-induced damage to cultured HaCaT keratinocytes and the skin of hairless mice, PLoS One 9(5) (2014) e96804.

[2] Z. Janjetovic, S.G. Jarrett, E.F. Lee, C. Duprey, R.J. Reiter, A.T. Slominski, Melatonin and its metabolites protect human melanocytes against UVB-induced damage: Involvement of NRF2-mediated pathways, Sci Rep 7(1) (2017) 1274.

[3] Z. Janjetovic, M.A. Zmijewski, R.C. Tuckey, D.A. DeLeon, M.N. Nguyen, L.M. Pfeffer, A.T. Slominski, 20-Hydroxycholecalciferol, product of vitamin D3 hydroxylation by P450scc, decreases NF-kappaB activity by increasing IkappaB alpha levels in human keratinocytes, PLoS One 4(6) (2009) e5988.

[4] A. Slominski, T.K. Kim, A.A. Brozyna, Z. Janjetovic, D.L. Brooks, L.P. Schwab, C. Skobowiat, W. Jozwicki, T.N. Seagroves, The role of melanogenesis in regulation of melanoma behavior: melanogenesis leads to stimulation of HIF-1alpha expression and HIF-dependent attendant pathways, Arch Biochem Biophys 563 (2014) 79-93.

[5] A.T. Slominski, T.K. Kim, J.V. Hobrath, Z. Janjetovic, A.S.W. Oak, A. Postlethwaite, Z. Lin, W. Li, Y. Takeda, A.M. Jetten, R.C. Tuckey, Characterization of a new pathway that activates lumisterol in vivo to biologically active hydroxylumisterols, Sci Rep 7(1) (2017) 11434.

[6] A.T. Slominski, M.A. Zmijewski, B. Zbytek, A.A. Brozyna, J. Granese, A. Pisarchik, A. Szczesniewski, D.J. Tobin, Regulated proenkephalin expression in human skin and cultured skin cells, J Invest Dermatol 131(3) (2011) 613-22.